Effect of Copper and Copper oxide Nanoparticles on The Transient Creep Properties of Sn-4Zn alloy

Mahmoud Y. Salem[1], Manal A. Maher[2*]

1.Head of Physics Department, Faculty of Science, New Valley University, New Valley 72511, El-Kharga, Egypt.

2. Faculty of Nanotechnology for Postgraduate Studies, Cairo University, Sheikh Zayed, Egypt; Computed Tomography X-ray Unit, Cairo Egyptian Museum, Ministry of Antiquities, Egypt.

Receive Date: 2022-08-08; Revise Date: 2022-09-21; Accept Date: 22 September 2022; Publish: 23 September 2022

Abstract

Cu-Sn-Zn alloys are excessively utilized in different manufacturing applications due to their unparalleled advantages, such as very its low resistivity, altitude business strength, and premium weld ability. Sn-4Zn alloy is concerning to the lead-liberation arrangement which is favourable in respect of the comparatively minimal fusion degree and minimal price. Nevertheless, Zn displays destitute oxidation and corrosion resistance which prevent welding employment. The present research studied the addition effect of Cu and CuO nanoparticles (NPS) on the transient creep properties of the Sn-4Zn alloy. Three compositions of Cu-Sn-Zn alloys were studied Sn-4Zn, Sn-4Zn-0.4CuO (NPS), and Sn-4Zn-1.5Cu (NPS). X-ray diffraction (XRD) and Scanning Electron Microscopy attached with Energy-dispersive X-ray spectroscopy (SEM-EDX) were used to investigate the microstructure of the prepared alloy samples. The results proved the addition of 0.4 CuO (NPS) to Sn-4Zn alloy increased the strength of the alloy by about 11%, while the addition of 1.5 Cu (NPS) increased the ductility of the alloy by about 14%. Additionally, the Creep property for Sn-4Zn; Sn-4Zn-0.4 CuO (NPS), and Sn-4Zn-1.5Cu (NPS)

* Corresponding author: *E-mail address*: manal.a.maher@gmail.com

alloys is investigated during distinct employing temperatures, three degrees extended between 303 until 373 K and under seven varied fixed utilized stresses (σ) from 10 MPa to 24 MPa. The results showed the magnitude of β and n is distinctly linked to the creep test circumstances (T) and stress (σ) as $\varepsilon tr = \beta tn$. The coefficients (n) is raised by rising (T) regardless of the utilized stress (σ); while (β) is reduced by growing (T) and /or stress (σ).

Keywords: Cu nanoparticles; CuO Nanoparticles; Sn-4Zn alloys, Transient creep mechanical property.

1. Introduction:

The ternary alloy Cu-Sn-Zn (CSZ) has great workable advantages and they are excessively utilized for most industrial applications, this is because of its unparalleled advantages such as its very low resistivity, premium weldability, comprehensive wonderful appearance, and high rustiness strength [1,2], additionally, its noticeable capability property and its very low resistivity [3,4]. Generally, Sn-Zn alloy is a unit concerning to the lead-liberation arrangement which is favorable with respect to the comparatively minimal fusion degree and minimal price. Nevertheless, Zn displays a destitute oxidation and corrosion opposition which prevent the welding employment. The Cu-Sn-Zn alloy was prepared by different procedures such as the fusion method [5, 6], grinding materials [6] and electrostatic deposition [7, 8]. Also, it was excessively utilized for telecommunication apparatus because of its premium achievement for hot / electricity accessibility, welding ability, and abrasion resistance [8].

Cu and CuO nanoparticles are promising additives to Sn-4Zn alloy to reinforce its oxidation and reduction because they controlled the movement of the charge [9,10]. Moreover, the unprecedented CuO (NPS) which is synthesized by an adjusted water heated procedure for taking off requirement for materials, will be established the fundamental to a gas discoverer and display perfect amelioration for response to carbon monoxide (CO) sensor resemble to clear nanowires [11, 12]. Eventually, CuO (NPS) is feigned through ITO (Indium Tin Oxide) refined glass ingredients with throbbed laser precipitation [13]. Since CuO (NPS) can perform the oxidation and reduction properties and thus perform the non-attendance to every outer intercessor and the perfect redox crest which will be apparent in the device measuring. The refinement in the characteristics of Cu, CuO (NPS) is regarded as the lowering in the energy gap, and it was demonstrated that the elevation of the Cu ratio in the CuO Nanoparticle; tends to the minimal band gap [14]. Many researches illustrated that the CuO nano-composite demands ganglion manner, which includes altitude degree; an extended interval. CuO is synthesized using high reaction (at 673 °K for 720 min using 15% argon and 85% O_2 atmosphere); the Cu at first is created using a radio frequency (RF) sputtering apparatus [15,16]. Different characterization procedures were used to characterize CuO and ZnO nanocomposites. Works of the literature demonstrated that the nanoparticles which can include the three main ingredients (i.e. Sn, Zn, and Cu), dominate an essence-frame structure; also it manifested a condition arrangement assorted about an accumulation sample [17,18].

The susceptible composition of CuO nanowire (NW) samples also was elucidated which has an extremely maximum invader reaction (~ 340) than nanostructured films (~ 3) during the testing degrees about 573 °K. Since, the altitude gas reaction for CuO (NW) networks issue was demonstrated via penetrating stage commute of CuO (NW) layer to samples of Cu. This process was spot-check at a testing degree of more than 548 °K, however, it gave perfect repercussion about 573 °K. Near an altitude working degree around 673 °K, the gas reaction is presented minimum (~ 108) than about 573 °K, the reaction and nominating periods are very smaller [10,19].

The present work focused on the study of the influence of CuO and Cu nanoparticles on the transient creep properties of Sn-4Zn alloy. The study was performed on three different compositions of Sn-Zn alloys; Sn-4Zn, Sn-4Zn-0.4CuO (NPS), and Sn-4Zn-1.5Cu (NPS). The creep property was investigated in three different employing temperatures (T) ranging from 303 °K and 373 °K, and under seven varied fixed utilized stresses (σ) from 10 to 24 MPa.

2. Experimental Procedures:

2.1 Materials:

The ingredient metals and the nono-chemicals were purchased from the Sigma-Aldrich Company, as follows: nanopowder of copper oxide (CuO-NPs) < 50nm particle size, purity ≥ 99.0%, No: 24878789; nanopowder of copper (Cu-NPS) < 40-60 nm particle size, purity ≥ 99.5%, No.774111, Zn metal foil No.349410, thickness 1.0 mm, purity 99.99%, Sn metal foil No.265756, thickness 0.5 mm, purity 99.998%. The alloys Sn-4Zn, Sn-4Zn-0.4CuO (NPS), and Sn-4Zn-1.5Cu (NPS) were prepared by mixing the ingredient metals Sn, Zn with the chemicals Cu, CuO (NPS) under vacuum melting. Then, the ingots were wheeled to wires and annealed at 423 °K for 125 min which subsequently advisedly froze to 298 °K by rate T= 0.02 °K/sec. Worth mentioning, that before the test the prepared alloys were annealed at 298 °K for 10000 min. This thermal treatment licensed the tiny quantities of grain growth and grain stabilization to take place [20].

2.2 Characterization Methods:

The alloy microstructures were investigated using X-ray diffraction and SEM/EDX. Transient creep distortion was achieved on tested alloys of 0.8 mm diameters and 50 mm criterion range. The samples were tested at temperatures ranging from 303 °K to 373 °K under different strain rates ranging from 10 to 24 MPa, using a common computerized type creep machine [21, 22]. The precision of the degree range is ±1°C. Table 1 shows the elemental analysis of actual compositions of the tested alloy samples by wt. % by using Energy-dispersive X-ray spectroscopy (EDX).

Table (1): EDS elemental analysis of actual compositions of the experimental alloys by wt. %

Experimental	Sn %	Zn %	CuO %	Cu %
Sn-4Zn	96	4	0	0
Sn-4Zn-0.4CuO	95.6	4	0.4	0
Sn-4Zn-1.5Cu	94.5	4	0	1.5

3. Results and Discussion:

This work focused on studying the effect of the addition of Cu and CuO nanoparticles (NPS) on the transient creep of the alloy Sn-4Zn. Three alloy samples were prepared Sn-4Zn, Sn-4Zn-0.4CuO (NPS), and Sn-4Zn-1.5Cu (NPS). Figure 1 (a-c) shows X-ray diffraction patterns for the three alloys Sn-4Zn; Sn-4Zn-0.4CuO (NPs); and Sn-4Zn-1.5Cu (NPS) were crept at 333 °K and under 14 MPa. The figures show the chemical composition of the three tested alloys by using the Joint Committee on Powder Diffraction Standards (JCPDS) of Cu-4Zn (file no.28-1486), Sn (file no.04-0673), Zn (file no.04-831), CuO (file no.05-661) and Cu (file no.04-836). Figure 2a shows CuO in the microstructure of Sn-4Zn-0.4CuO (NPS) alloy in the white phase, while the Sn-4Zn phase appears in black as shown in Figure 2b. Figure 2c shows the microstructure of Sn-4Zn-1.5Cu (NPS) alloy, the content of Cu was added to improve the microstructure and the mechanical properties of the prepared alloy. Additionally, Cu content is able to refine the grain size, and the Cu_5Zn_8 phase act as heterogeneous nucleation sites for β-Sn dendrites structure which solidify the alloy, besides the existence of the CuO phase which appears in white color. This ternary refine grain size microstructure resulted in more strain than the other alloys.

Figures 4-6 show the isothermal transient creep curves of the three samples at different temperatures 303 °K, 333 °K, and 373 °K respectively, and under different seven applied stresses ranging from 10 to 24 MPa. Also, Figure 7 (a, b) shows a comparison of the creep curves at temperatures 333 °K and 373 °K of the three alloy samples at applied stresses 10 MPa and 24 MPa. It is obvious the creep curve of the alloy Sn-4Zn-0.4CuO (NPS) at 333 °K and applied stress of 10 Mpa is less strain than Sn-4Zn-1.5Cu (NPS), while the alloy sample of Sn-4Zn has intermediate value. When tested samples at 373K and under applied stress of 24 MPa, it can be seen that the three ternary alloys have more elongation. The alloys which contain nanoparticles in their structures have small elongation. Since the association of 0.4 CuO (NPS) gives considerable leverage as low ductility and more strengthening than Sn-4Zn alloy by 11%. While the addition of 1.5Cu (NPS) to the alloy of Sn-4Zn increased the ductility of the resulting ternary alloy by 14%. It is obvious these isothermal creep curves are sensitive to both the deformation temperature, T, and the applied stress, σ, and they also show a monotonic shift towards higher strains and lower fracture times with increasing the deformation temperature. Thus, the level of creep strain for a ternary alloy is generally higher than a binary alloy, especially which was containing nanoparticles under the same test conditions. Subsequently, the transient creep strain, (εtr) was instituted in a related form [23].

$$\textbf{Strain transient} = \textbf{Beta} * \textbf{creep time}^{\,n} \qquad (1)$$

Where time is the transient creep time and Beta, n, are constants depending on the test conditions.

Figures (8-10) show the relation between (lnεtr) and (lnt) at 303 °K, 333 °K, and 373 °K temperatures respectively, and under different seven applied stress values ranging between 10 and 24MPa. The strain rate ranges from 9.7×10^{-6} to 13×10^{-6} for and from 1.0×10^{-5} to 16×10^{-3} for Sn-4Zn and from 5.0×10^{-6} to $55 \times 10^{-}$

^{3} for Sn-4Zn-1.5Cu (NPS) see Figures (11, 12). Table (2) shows a comparison of the transient creep of the tested three alloys. Obviously, this comparison shows that Sn-4Zn-1.5Cu (NPS) is more elastic than the binary Sn-4Zn and Sn-4Zn-0.4CuO (NPS). The exponent, n, was evaluated using the inclination relate ln strain transient (lnst) and ln time (lnt), but the coefficient beta β was evaluated using the intercepts at ln time = zero. The results show the exponent n range from 0.58 to 1.6 to the Sn-4Zn binary alloy, while it ranges from 0.57 to 1.0 to the ternary Sn-4Zn-0.4CuO (NPS) alloy, and from 0.60 to 1.11 to the ternary alloy Sn-4Zn-1.5Cu (NPS). Figure 10 shows the dependence of the parameters, n, on the working temperature at different applied stresses for Sn-4Zn-0.4CuO (NPS); Sn-4Zn; and Sn-4Zn-1.5Cu (NPS). Whereas, it was found the value of n increases by increasing the deformation temperature and the applied stresses for the three alloys. While, Figure 13 shows the dependence of the parameters, β, on the working temperature at different applied stresses for Sn-4Zn; Sn-4Zn-0.4CuO (NPS); Sn-4Zn-1.5Cu (NPS). Since, It was found the parameter, β, raises with increased temperature and applied stress, it was found to exhibit appreciations ranging from -12.00 to - 4.94 for Sn-4Zn alloys, while it ranges from -12.77 to -5.92 for the Sn-4Zn-0.4CuO (NPS) alloy, and from -10.89 to -3.58 for the Sn-4Zn-1.5Cu (NPS) alloy. So, it was found that n, and coefficient,β, increase by increasing misrepresentation degree and loads.

Table (2): Comparison of the transient creep characteristics of the tested alloys

Experimental alloys	Exponent (n)	Coefficient (β)	Strain rate ($\dot{\varepsilon}$)
Sn-4Zn	0.58 : 1.6	-12.00 : -	$1.0x10^{-5}$: $16x10^{-3}$
Sn-4Zn-0.4CuO	0.57 : 1.0	-12.77 : -	$9.7x10^{-6}$: $13x10^{-6}$
Sn-4Zn-1.5Cu	0.60 : 1.11	-10.89 : -	$5.0x10^{-6}$: $55x10^{-3}$

Where time is the transient creep time and Beta, n, are constants depending on the test conditions.

It is obvious the stress, n, and the temperature dependence, β, showed a rapid increase at high temperatures in the three prepared alloys. Also, it is seen that under the same test conditions the ternary alloys with nanoparticles have so high yield creep rates compared to those of alloy binary. The relation between the coefficient β and the strain rate of the steady state creep ($\dot{\varepsilon}St$) were given by the equation [24].

$$\textbf{Beta} = (\textbf{Beta})_0\ (\textbf{strain steady})^{\gamma} \qquad (3)$$

Where, $(Beta)_0$ and γ are constants with respected to the experimental conditions.

Figure 15 shows the relation between the dependence of the parameters, Lnβ and lnε.st on the working temperature at different applied stresses for the three alloys Sn-4Zn-0.4CuO (NPS); Sn-4Zn; and Sn-4Zn-1.5Cu (NPS). The figure shows γ ranges from 0.08 to 0.083 for Sn-4Zn binary alloys, while it ranges between 0.04 to 0.08 for the ternary alloy Sn-4Zn-0.4CuO (NPS) alloy and from 0.083 to 0.119 for Sn-4Zn-1.5Cu (NPS). Depended on these results the alloy Sn-4Zn-0.4CuO (NPS) alloy is more strengthening than the other two other alloys; while the alloy Sn-4Zn-1.5Cu is more softening than the two other samples.

$\ln beta = \{(\ln time_2\ strain_{transient1} - \ln time_1\ strain_{transient2}) / (\ln time_2 - \ln time_1)\}$(2) The activation energy of the transient creep of three alloys was calculated using an Arrhenius equation of the form [25-29].

$$K=e^{-E/(RT)}$$

k : the rate constant.

T : the absolute temperature (in kelvins).

A : a constant due to frequency of collisions in the correct orientation.

E : the activation energy in Joules/mol.

R : the universal gas constant.

Figure 16 shows the activation energy (relation between Lnεtr and 1000/T) at different applied stresses for the alloys Sn-4Zn; Sn-4Zn-0.4CuO (NPs); and Sn-4Zn-1.5Cu (NPS) at un-equable loads. It is obvious the activation energies for Sn-4Zn-0.4CuO (NPS) are exceeding those of the binary Sn-4Zn and the ternary alloys Sn-4Zn-1.5Cu (NPs). This result indicates that the alloys containing CuO nanoparticles are exceedingly strengthening than the other two alloys, while the ternary alloy containing Cu nanoparticles is exceedingly elastic and the binary Sn-4Zn alloy has a mediate strain. This might be due to the refining effect of Zn which prevents the formation of low strength of the small structure in the ternary alloy and needs lower energies than the binary alloy and which contains nanoparticles.

4. Conclusions:

The present work investigated the influence of Cu and CuO nanoparticles on Transient Creep Characteristics of Sn-4Zn alloy. Three alloys were studied Sn-4Zn, Sn-4Zn-0.4CuO (NPs), and Sn-4Zn-1.5Cu (NPs); the results will be concluded as follows:

(1) This study proved the addition of 0.4 CuO (NPS) increase the strengthening of the alloy Sn-4Zn by the value of 11%, so the resulted alloy will be low ductility. While the addition of about 1.5Cu (NPS) increases the ductility of Sn-4Zn alloy by about 14%.

(2) Also, the study pronounced that at the experiential conditions 333 °K and 10 MPa the alloy Sn-4Zn-0.4CuO (NPS) is less strained, while Sn-4Zn-1.5Cu (NPS) has exceedingly strained and Sn-4Zn has intermediate estimation.

(3) The results showed the isothermal creep curves are sensitive to the deformation temperature, T, and the applied stress, σ. Also, it showed a monotonic shift towards higher strains and lower fracture times with increasing the deformation temperature.

(4) The results showed the strain rate from 9.7x10^{-6} to 13x10^{-6} for Sn-4Zn-0.4CuO (NPs), and from 1.0x10^{-5} to 16x10^{-3} for Sn-4Zn and from 5.0x10^{-6} to 55x10^{-3} for Sn-4Zn-1.5Cu (NPs). Thus, these values show that Sn-4Zn-1.5Cu (NPS) is more elastic than the binary Sn-4Zn and the ternary Sn-4Zn-0.4CuO (NPs).

(5) Finally, the results showed the activation energies for Sn-4Zn-0.4CuO (NPS) are exceeding than for the binary alloy Sn-4Zn and the ternary alloy Sn-4Zn-1.5Cu (NPs). This result corroborative that the alloys which contain CuO nanoparticles are exceedingly strengthening than the other two tested alloys; while the binary alloy Sn-4Zn has intermediate strain.

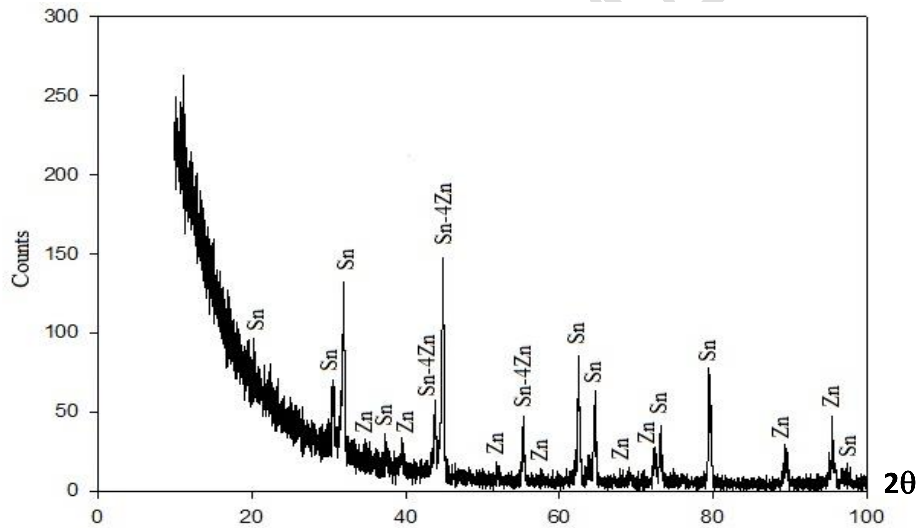

a

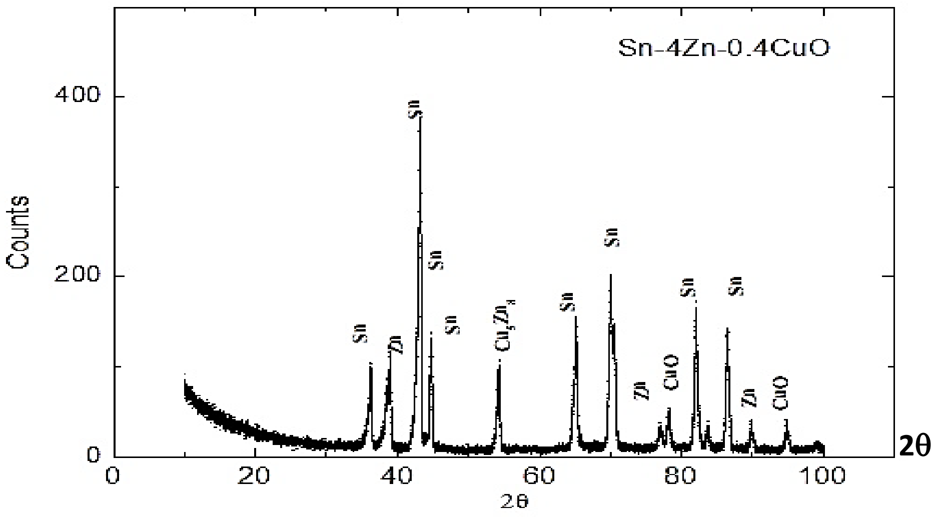

b

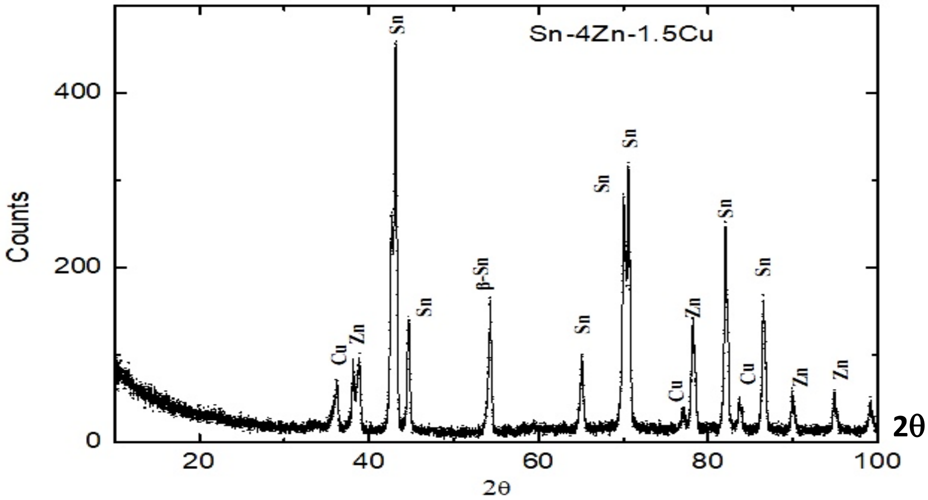

C

Figure 1 (a-c) X-ray diffraction patterns for the tested samples for Sn-4Zn; Sn-4Zn-0.4CuO (NPs), Sn-4Zn-1.5Cu (NPS) were crept at 333 K and 14 MPa, the Joint Committee on Powder Diffraction Standards (JCPDS) of Cu-4Zn (file no.28-1486), Sn (file no.04-0673), Zn (file no.04-831), CuO (file no.05-661) and Cu (file no.04-836)

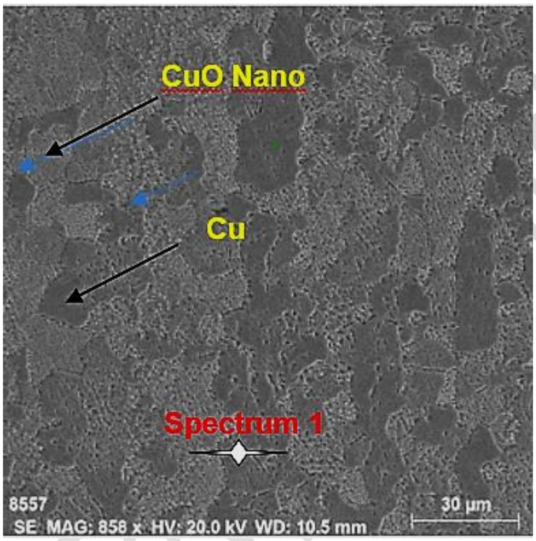

a

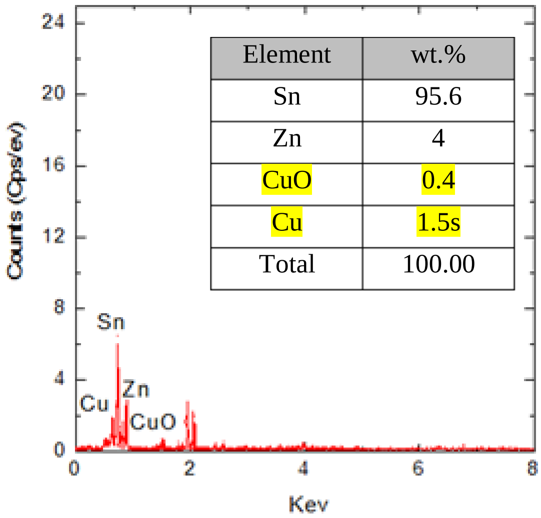

Element	wt.%
Sn	95.6
Zn	4
CuO	0.4
Cu	1.5s
Total	100.00

b

Figure 2. (a,b) SEM micrograph and EDX pattern of the tested alloy Sn-4Zn-1.5Cu was crept at 333 °K and 14 MPa.

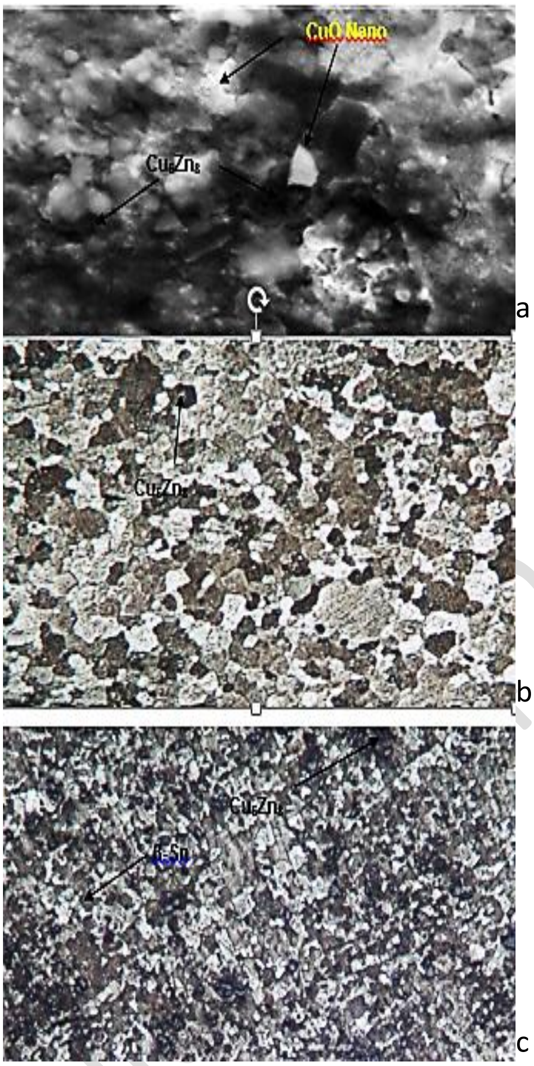

Figure 3. SEM micrographs of the deformed samples of Sn-4Zn; Sn-4Zn 0.4CuO (NPs), Sn-4Zn-1.5Cu (NPS) alloys which crept at 333°K and 14 MPa; (a) microstructure of Sn-4Zn-0.4CuO (NPS) CuO appear in white phase, while Cu_5Zn_8 appears in black colour; (b) Microstructure of Sn-4Zn appears in black colour; (c) fine microstructure of Sn-4Zn-1.5Cu (NPS)

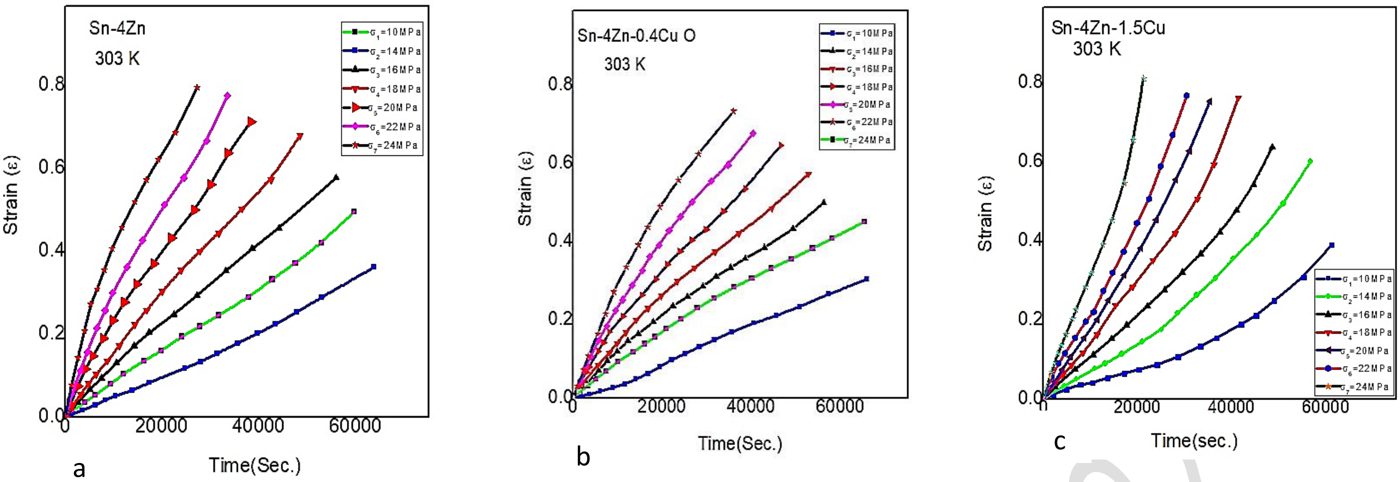

Figure 4. Isothermal Creep curves at 303 °K and different applied stresses for Sn-4Zn; Sn-4Zn-0.4CuO (NPs), Sn-4Zn-1.5Cu (NPs)

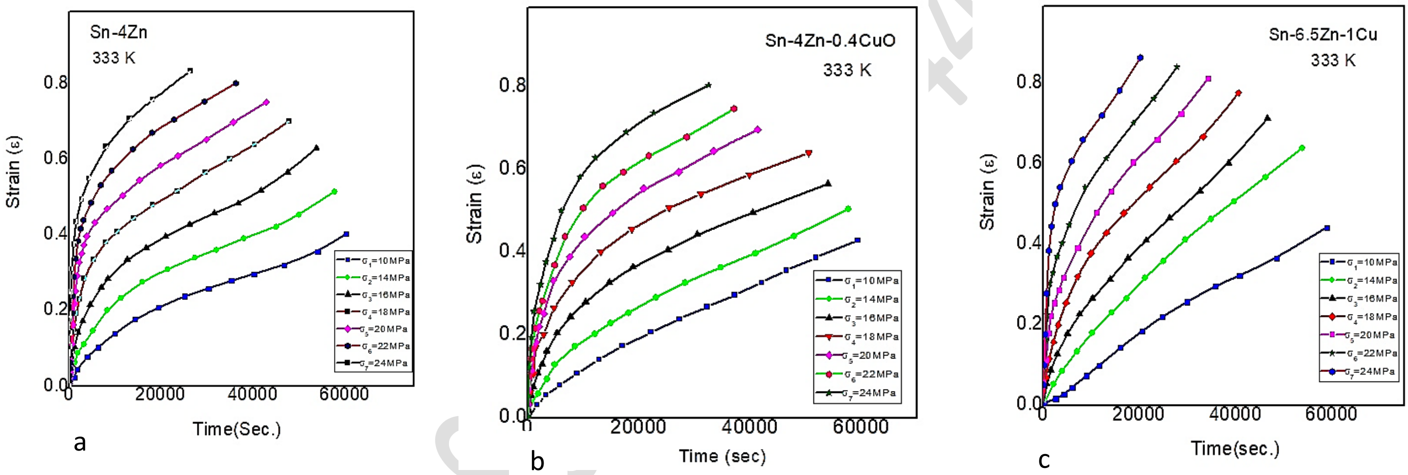

Figure 5. Isothermal Creep curves at 333 °K and different applied stresses for Sn-4Zn; Sn-4Zn-0.4CuO (NPs), Sn-4Zn-1.5Cu (NPs)

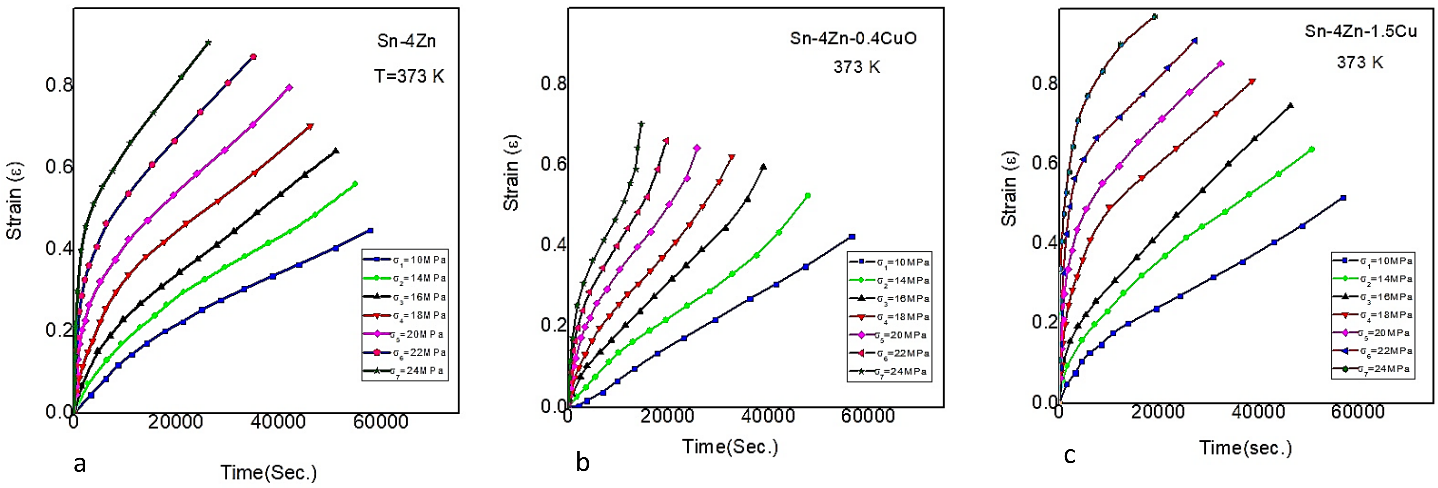

Figure 6. Isothermal Creep curves at 373 °K and different applied stresses for Sn-4Zn; Sn-4Zn-0.4CuO (NPs), Sn-4Zn-1.5Cu (NPs)

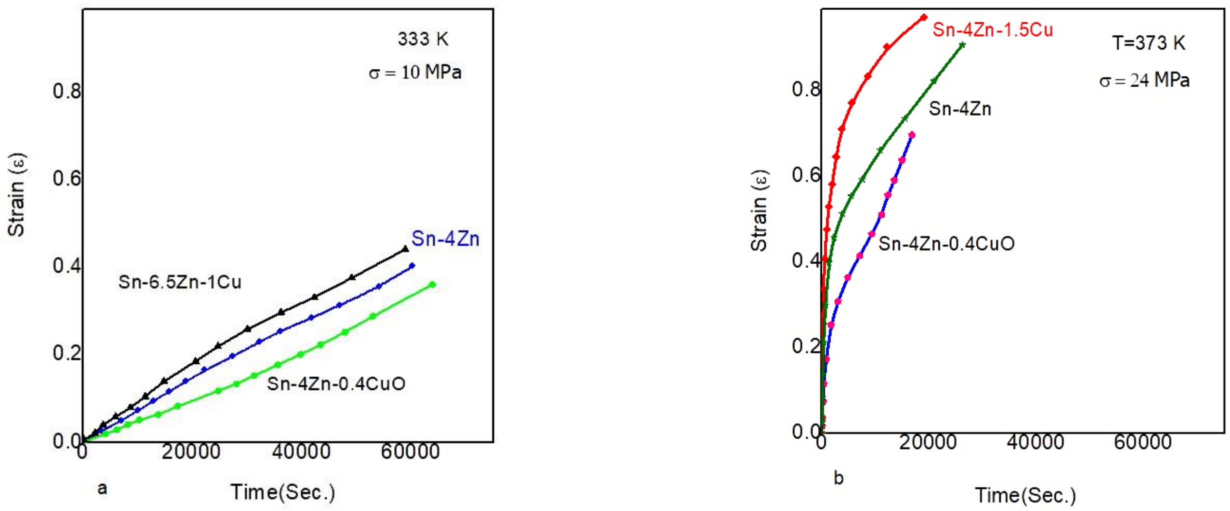

Figure 7. Comparison of Creep Curves at 333 °K and 373 °K at applied stresses 10 MPa and 24 MPa for Sn-4Zn; Sn-4Zn-0.4CuO (NPs), Sn-4Zn-1.5Cu (NPs)

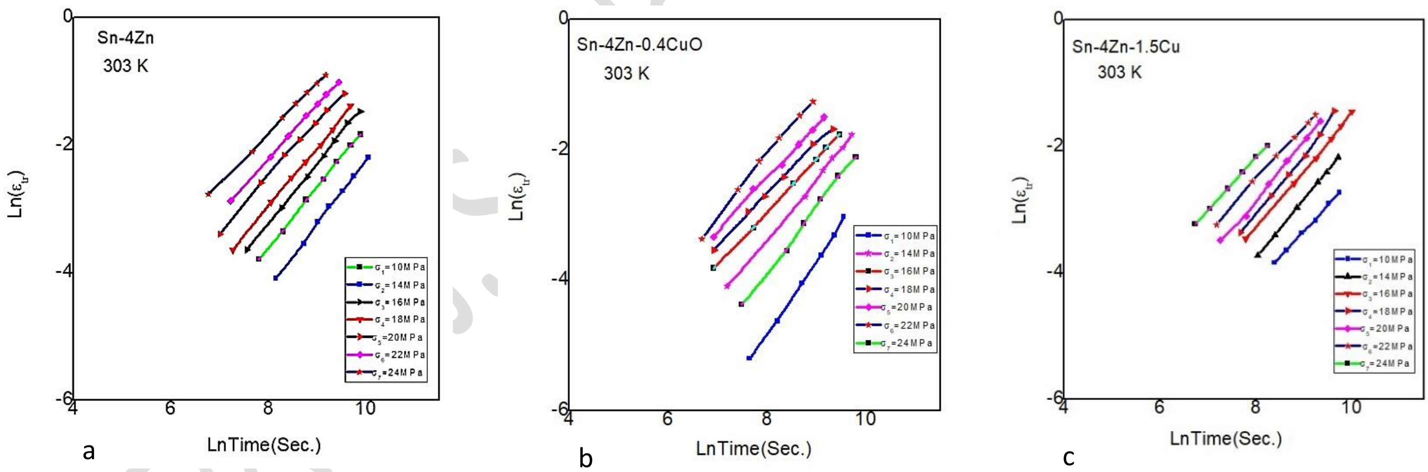

Figure 8. Relation between lnεtr and lnt for Sn-4Zn; Sn-4Zn-0.4CuO (NPs), Sn-4Zn-1.5Cu (NPS) at 303 °K and different stresses

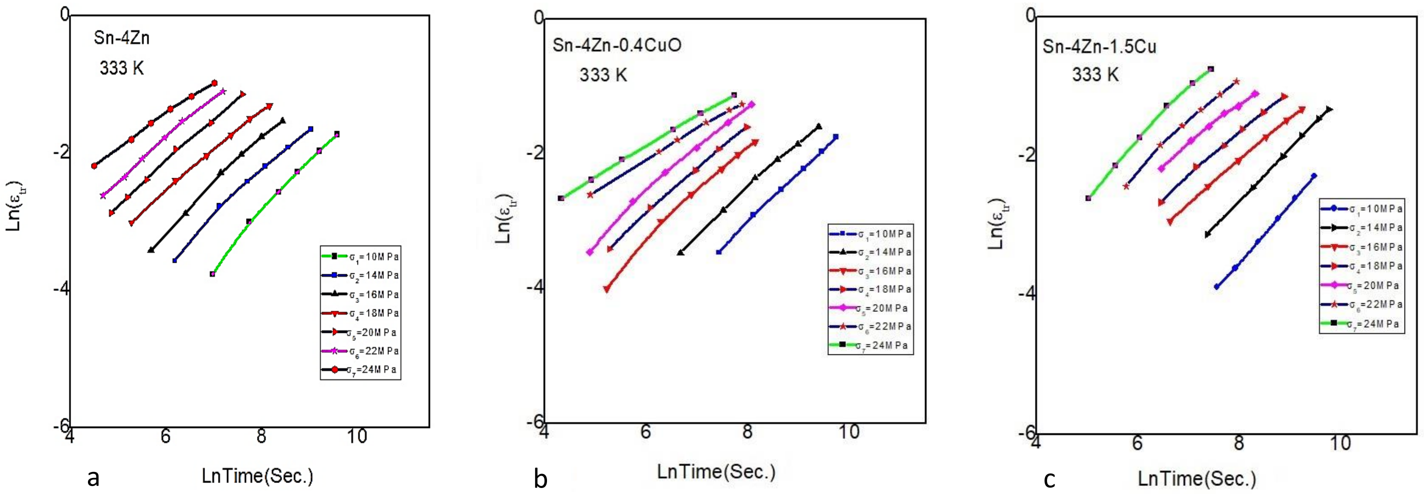

Figure 9. Relation between lnεtr and lnt for Sn-4Zn; Sn-4Zn-0.4CuO (NPs), Sn-4Zn-1.5Cu (NPS) at 333 °K and different stresses

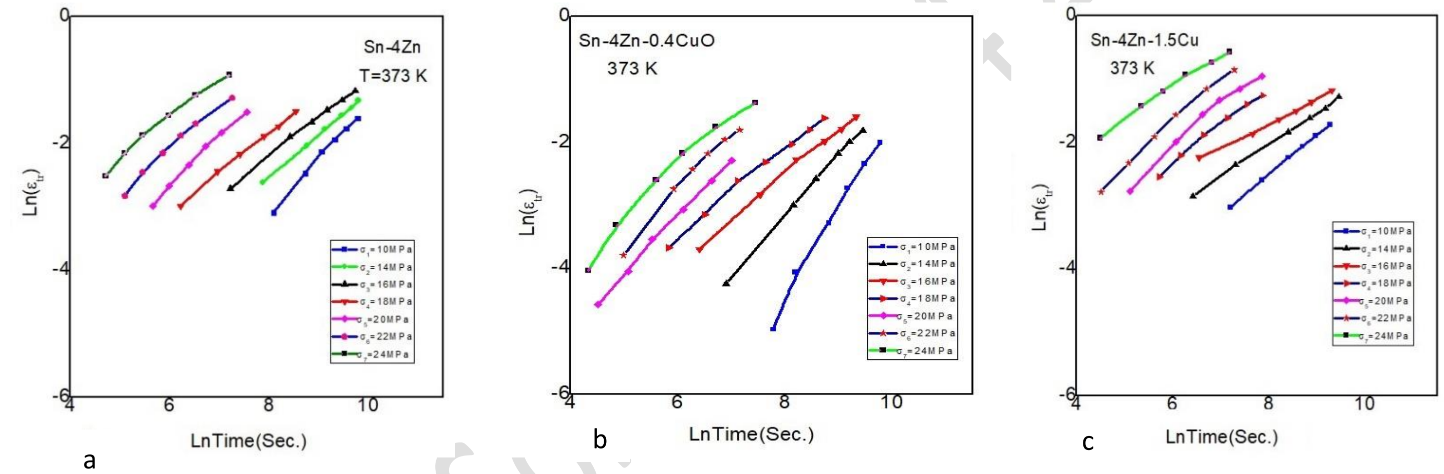

Figure 10. Relation between lnεtr and lnt for Sn-4Zn; Sn-4Zn-0.4CuO (NPs), Sn-4Zn-1.5Cu (NPS) at 373 °K and different stresses

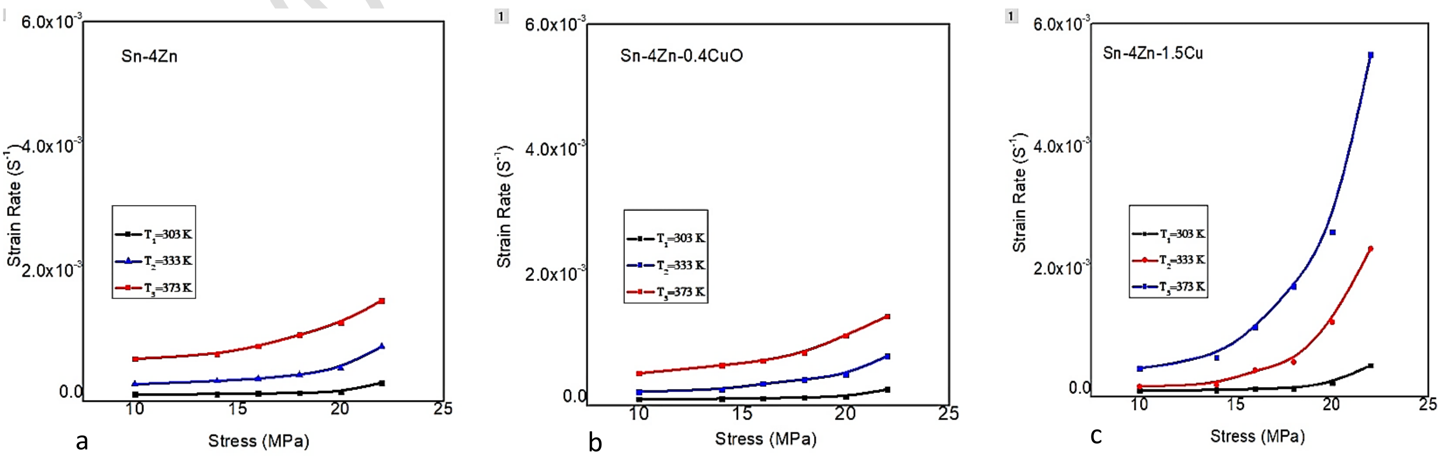

Figure 11. Comparison of Strain Rate (S^{-1}) for Sn-4Zn; Sn-4Zn-0.4CuO (NPs), Sn-4Zn-

1.5Cu (NPS) at different applied stresses curves at fixed tested degree

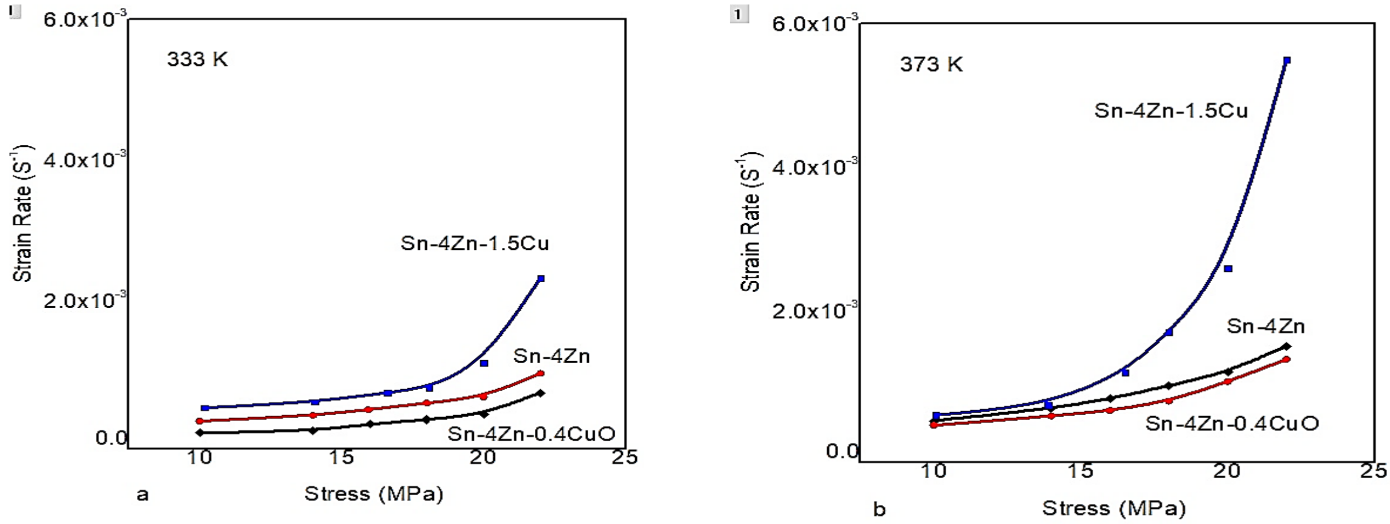

Figure 12. Comparison of Strain Rate (S^{-1}) at 333 °K and 373 °K, with different applied stresses for Sn-4Zn; Sn-4Zn-0.4CuO (NPs), Sn-4Zn-1.5Cu (NPs)

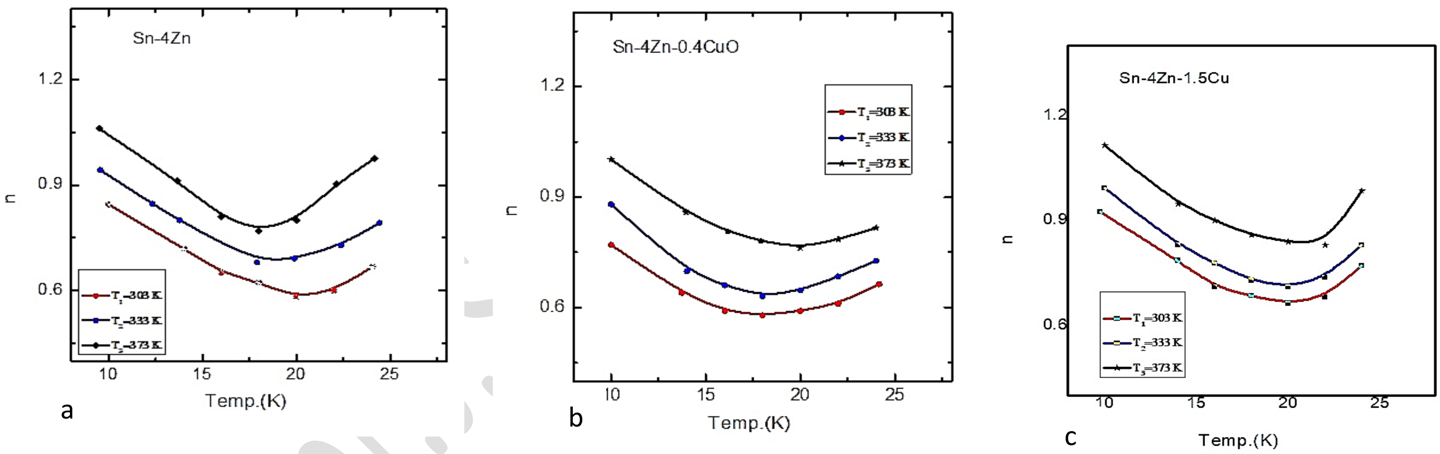

Figure 13.The dependence of the parameters, n, on the working temperature at different applied stresses for Sn-4Zn; Sn-4Zn-0.4CuO (NPs), Sn-4Zn-1.5Cu (NPs)

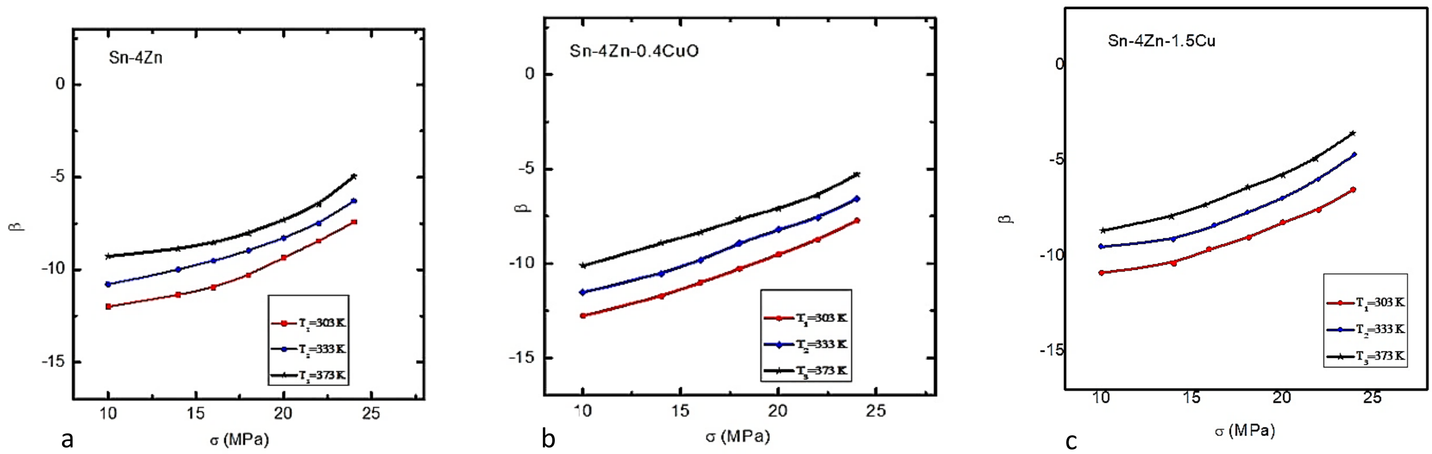

Figure 14.The dependence of the parameters, β, on the working temperature at different applied stresses for Sn-4Zn; Sn-4Zn-0.4CuO (NPs), Sn-4Zn-1.5Cu (NPs)

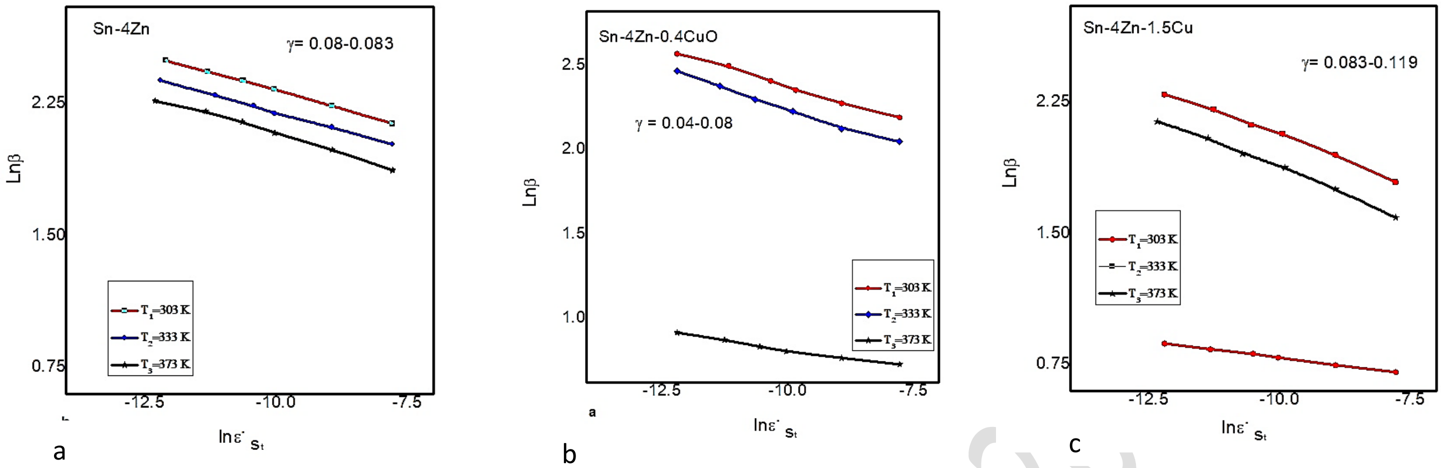

Figure 15.The relation between Lnβ and lnε.st for Sn-4Zn; Sn-4Zn-0.4CuO (NPs), Sn-4Zn-1.5Cu (NPs)

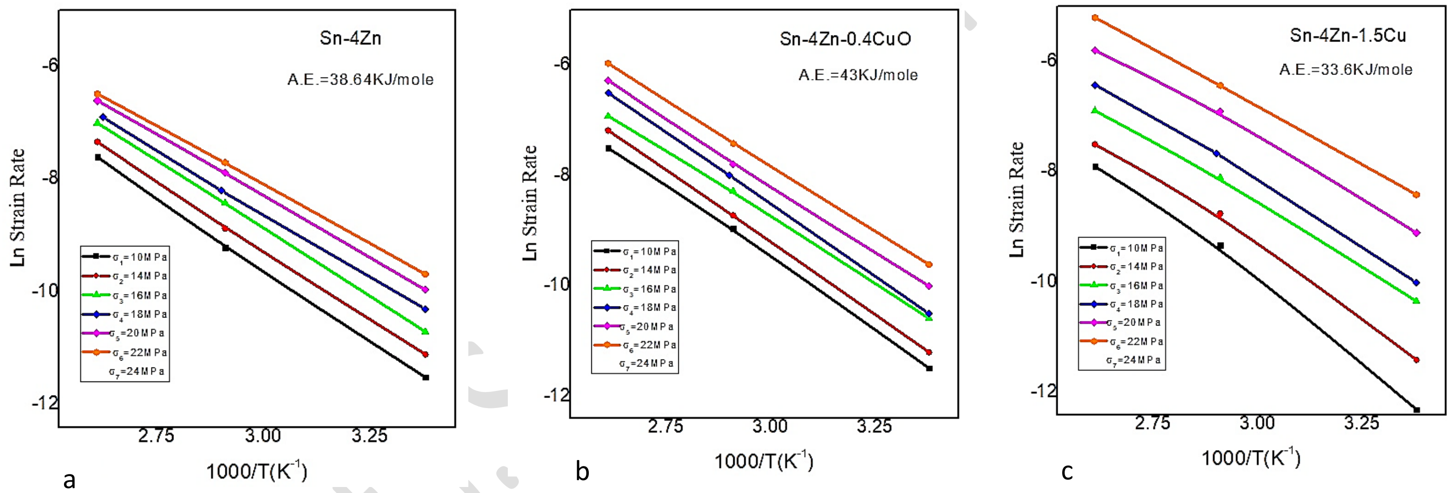

Figure16. The activation energy (relation between Lnε.tr and 1000/T) at different applied stresses for Sn-4Zn; Sn-4Zn-0.4CuO (NPs), Sn-4Zn-1.5Cu (NPs)

References:

[1] G. Weidong, et al., Microstructure and properties of Cu-Sn-Zn-TiO_2 nano-composite coatings on mild steel. Surface and Coatings Technology **350** (2018): 801-806. https://doi.org/10.1016/j.surfcoat.2018.04.046

[2] A., Brenner, Electrodeposition of alloys: principles and practice. General survey, principles, and alloys of copper and of silver. Academic Press, 1963. https://onlinelibrary.wiley.com/doi/abs/10.1002/bbpc.19640680319

[3] F. C. Walsh, and C. T. J. Low. "A review of developments in the electrodeposition of tin-copper alloys." Surface and Coatings Technology **304** (2016): 246-262. https://doi.org/10.1016/j.surfcoat.2016.06.065

[4] S. C. Yang, et al. "Strong Zn concentration effect on the soldering reactions between Sn-based solders and Cu." Journal of materials research **21**.10 (2006): 2436-2439. https://doi.org/10.1557/jmr.2006.0320

[5] M. Date, et al. "Interfacial reactions and impact reliability of Sn–Zn solder joints on Cu or electroless Au/Ni (P) bond-pads." Journal of Materials Research **19**.10 (2004): 2887-2896. https://doi.org/10.1557/JMR.2004.0371

[6] M. Yang, et al. "Development of Sn-Zn-Cu lead free solder, "11th International Conference on Electronic Packaging Technology & High Density Packaging. IEEE, 2010. 10.1109/ICEPT.2010.5582695

[7] Y. Chi-Yang, and D. Jenq-Gong "Stabilization of hexagonal Cu6 (Sn, Zn) 5 by minor Zn doping of Sn-based solder joints." Scripta Materialia **65**. 9 (2011): 783-786. https://doi.org/10.1016/j.scriptamat.2011.07.029Get

[8] Y. Wang, et al. "Cu–Sn–Zn nanocomposite coatings prepared by TiO2 sol-enhanced electrodeposition." Journal of Applied Electrochemistry **50**. 8 (2020): 875-885. https://doi.org/10.1007/s10800-020-01442-z

[9] C. Lu, et al. "A copper oxide/zinc oxide composite nano-surface for use in a biosensor." Materials 12.7 (2019): 1126. https://doi.org/10.3390/ma12071126

[10] T. Ai Ting, T. Ai Wen, and Y. Farazila "Influence of nanoparticle addition on the formation and growth of intermetallic compounds (IMCs) in Cu/Sn–Ag–Cu/Cu solder joint during different thermal conditions." Science and technology of advanced materials (2015). https://doi.org/10.1088/1468-6996/16/3/033505

[11] J. X. Wang, et al. "Free-standing ZnO–CuO composite nanowire array films and their gas sensing properties." Nanotechnology 22.32 (2011): 325704. http://iopscience.iop.org/0957-4484/22/32/325704

[12] R. A. Ismail; Investigation of Microstructure and Mechanical Properties of Different Nano - Particles Doped Sn-Zn Lead-Free Solder Alloys; Article 20, Volume **53**, Issue 1, winter 2020: 191-199.

[13] N. Batra, et al. "ZnO–CuO composite matrix based reagentless biosensor for detection of total cholesterol." Biosensors and Bioelectronics **67** (2015): 263-271. https://doi.org/10.1016/j.bios.2014.08.029

[14] N. Widiarti, J. Sae, and S. Wahyuni. "Synthesis CuO–ZnO Nanocomposite and Its Application as an Antibacterial Agent. IOP Conference Series: Materials Science and Engineering." (2017): 012036. IOP Conf. Series: Materials Science and Engineering 172 (2017) 012036 doi:10.1088/1757-899X/172/1/012036

[15] D. Zappa, S. Dalola,; G. Faglia; E. Comini,; M. Ferroni,; C. Soldano,; V. Ferrari,; G. Sberveglieri, Integration of ZnO and CuO nanowires into a thermoelectric module, *Beilstein J. Nanotechnol*. 2014, 5, 927–936. doi:10.3762/bjnano.5.106

[16] F. Glöckel et al. "Influence of Zn and Sn on the precipitation behavior of new Al–Mg–Si alloys." Materials 12.16 (2019): 2547. https://doi.org/10.3390/ma12162547

[17] A. Roshanghias, B. Johannes, and I. Herbert, "An attempt to synthesize Sn-Zn-Cu alloy nanoparticles." Materials Letters **178** (2016): 10-14. https://doi.org/10.1016/j.matlet.2016.04.192

[18] O. Olkhovych, et al. "The effect of copper and zinc nanoparticles on the growth parameters, contents of ascorbic acid, and qualitative composition of amino acids and acylcarnitines in Pistia stratiotes L.(Araceae)." Nanoscale Research Letters **11.1** (2016): 1-9. https://doi.org/10.1186/s11671-

016-1422-9

[19] O. Lupan, et al. "Influence of CuO nanostructures morphology on hydrogen gas sensing performances." Microelectronic Engineering **164** (2016): 63-70. https://doi.org/10.1016/j.mee.2016.07.008

[20] Kenawy MA, Sakr MS, Sakr EM, Zayed HA, and Mourad NO. Transient and Steady State Creep of Al 4.5 wt% Mg During Phase Transformation. 1990: phys. stat. sol. (a) 121, 467. https://doi.org/10.1002/pssa.2211210214

[21] A.A. El-Daly, A.Z. Mohamad, A. Fawzy, A.M. El-Taher, Creep behavior of near-peritectic Sn–5Sb solders containing small amount of Ag and Cu, *Mater. Sci. Eng. A*, **528**, 1055 (2011). https://doi.org/10.1016/j.msea.2010.11.001

[22] M.Y. Salem, A.Z. Mohamed. "Transient creep characteristics of Tin Base Alloy", American Research Journal of Physics, vol. **4**, no. 1 (2011): pp. 1-12. www.arjonline.org

[23] M. Y. SALEM, "Influence of Cu Addition on the Transient Creep Characteristics of Sn–9Zn-1.5 Ag Solder Alloy." *American Research Journal of Physics*, vol. **6** (2020): 1-11. www.arjonline.org

[24] S. M. Alogla, and V. Kodur. "Temperature-induced transient creep strain in fiber-reinforced concrete." Cement and Concrete Composites **113** (2020): 103719. https://doi.org/10.1016/j.cemconcomp.2020.103719

[25] S. S pigarelli, and P. Chiara. "A unified physical model for creep and hot working of Al-Mg solid solution alloys." Metals **8.1** (2017): 9. https://doi.org/10.3390/met8010009

[26] M. E. Kassner and M-T. Pérez-Prado. "Five-power-law creep in single phase metals and alloys." Progress in materials science **45.1** (2000): 1-102. DOI:10.1016/B978-008043637-1/50003-X